Journal of Thermal Science Vol.29, No.4 (2020) 1001−1009

https://doi.org/10.1007/s11630-020-1331-1 **Article ID: 1003-2169(2020)04-1001-09**

Experimental Study on Thermal Management of Cylindrical Li-ion Battery with Flexible Microchannel Plates

WEI Liting[1,2], JIA Li[1,2*], AN Zhoujian[1,2], DANG Chao[1,2]

1. Institute of Thermal Engineering, School of Mechanical, Electronic and Control Engineering, Beijing Jiaotong University, Beijing 100044, China
2. Beijing Key Laboratory of Flow and Heat Transfer of Phase Changing in Micro and Small Scale, Beijing 100044, China

Abstract: A novel thermal management system of cylindrical Li-ion battery with the liquid cooling in flexible microchannel plate was established in the study. The experiments were conducted with R141b in flexible microchannel plates. The cooling system with the flexible aluminum microchannels can effectively transfer heat from battery to the cooling refrigerant R141b based on flow boiling. A battery module with five cells along flow channel was chosen to study the effects of contact surface area and mass flux on the thermal performance and electrochemical characteristics in the experiments. Three types of structure with different contact areas were studied and their performances were compared with the experiments without cooling structures. The experiments were carried out at the same discharge rate with the inlet mass flow rates of 0–10 kg/h. For the inlet mass flow rate of 5.98 kg/h, the surface temperature and temperature uniformity of battery were the best, and the output voltage and capacity of batteries were higher than those under other mass flow rates. With given inlet mass flow rates, the five series cells exhibited different electrochemical performances, including output voltage and discharge capacity, due to the different refrigerant flow states in the microchannels. Finally, an optimal design was presented with thermal performances, macroscopic electrochemical characteristics, inlet mass flow rates and cooling performance taken into consideration.

Keywords: thermal management, Li-ion battery, flexible microchannels, contact area

1. Introduction

For electric vehicles and hybrid vehicles, the power battery is the most important factor restricting the performance of electric vehicles [1]. Lithium-ion cells offer excellent energy conversion and storage for a variety of applications, including consumer electronics, electric vehicles and military electronics [2, 3]. However, the application of Li-ion cells has been severely limited by the concerns over overheating during operation [4]. Besides reduced performance and reliability at high temperatures, a serious safety concern was also presented [5]. Once the cell temperature exceeds a certain threshold, a series of exothermic processes occur within a Li-ion cell, including thermal runaway, capacity and power fade.

There are four main types of Battery Thermal Management Systems (BTMS) which include air cooling,

Received: Oct 14, 2019 AE: YUAN Yanping Corresponding author: JIA Li E-mail: ljia@bjtu.edu.cn

heat pipe cooling, phase change materials cooling (PCMs) and liquid cooling. The air-based lithium-ion battery cooling technology, which allows air to sweep across the battery pack to cooling battery, is widely used in battery cooling technology. Air cooling includes natural convection cool and forced convection cooling. Li et al. [6] compared the temperature distribution of battery module under different air velocities. In their research, the increase of maximum temperature inside battery module was in the range of 3.6°C to 12°C. The maximum temperature difference increased from 0.5°C to 3.5°C, when the air velocity decreased from 5 m/s to 1 m/s. Zhu et al. [7] analyzed an active thermal management system with a pure air-cooling mode, and concluded that the effect of cooling flow rate on the temperature rise had a significant effect for all discharge rates. Mohammadian et al. [8] compared the effect of air duct with or without fins and the fin height on the cooling effect of batteries. The results showed that the cooling effect could be improved obviously by adding fins in the air duct, and the uniformity of fin height also affected the temperature uniformity of the battery. Sum et al [9] simulated the battery modules with different flow paths. The results showed that the maximum temperature and the temperature gradient of battery module could be greatly reduced by using Z-type cooling channel. However, air cooling is difficult to achieve a compact system structure, and the cooling capacity at high discharge rate cannot meet the battery thermal management requirements.

The heat pipe cooling has the advantages of high thermal conductivity and compact structure. To improve the overall performance of the system, it is necessary to consider the tightness of the contact between the evaporation section of heat pipe and the surface of battery, and the enhancement of the cooling capacity of the condensing section. Zhao et al. [10] studied the battery thermal management method of an aluminum plate heat pipe. The results showed that the angle of heat pipe had no effect on the cooling effect, and the cooling effect of spray cooling method was the best. Rao et al. [11, 12] designed a battery thermal management system based on pulsating heat pipe, which was proved that the layout of battery and the angle of pulsating heat pipe had some influence on the cooling performance. Park et al. [13] optimized the loop heat pipe used for the cooling of lithium batteries in military aircraft. For cylindrical Li-ion battery, few works have been done for tube or plate heat pipes.

Phase Change Material (PCM) cooling mainly utilizes the characteristics of low melting point and high latent heat of PCM, and the little temperature change or basically unchanged during the phase change process. Khateeb et al. [14] compared the heat dissipation effect of natural convection cooling, foam aluminum, PCM and PCM/foam aluminum in four cases. The heat dissipation effect of PCM/foam aluminum was the most obvious, and the maximum temperature of battery was 17.5°C lower than that with natural convection cooling. Rao et al. [15] indicated that the maximum temperature and maximum temperature difference of the battery module could be controlled at 45°C and 5°C respectively with foam copper/paraffin composite phase change material. As a kind of energy storage material, phase change material itself does not have the function of heat dissipation. When the phase change material completely melted, the whole system would fail and have no sustainability. So it must be equipped with an external cooling cycle system. In general, the system is complex and the overall weight is increased, which is also the main factor limiting the application of this thermal management technology in large battery packs. In addition, the flammability of phase change materials remains unresolved, and it is a fatal factor for its application in Li-ion battery thermal management.

Liquid cooling is a traditional form of cooling, which is the most efficient and widely used cooling technology in industry. Because the main heat transfer mode of liquid cooling is convective heat transfer and flow boiling, and the heat transfer is stronger than air convection, it may be more effective and efficient in solving the problem of battery overheating. An et al. [16] studied a new type of thermal management system based on flow boiling in mini-channels utilizing dielectric hydrofluoroether liquid with boiling point is 34°C. Zhen et al. [17] put forward a liquid cooling method with small channel cold plate.

An et al. [18] summarized the methods of battery thermal management, and pointed out that the selection of BTMS should consider the cooling demand and applications, and liquid cooling was suggested as the most suitable method for large-scale battery pack charged/discharged at higher C-rate and in high-temperature environment. Therefore, a refrigerant with the boiling point in the optimum operating temperature range of battery was selected as working fluid, and the system based on the boiling heat transfer could not only achieve the high efficiency of battery thermal management with a small mass flow rate, but also keep the good temperature consistency of battery pack. However, at present, there is little research on the thermal management of cylindrical batteries using flow boiling heat transfer technology with flexible microchannels.

A thermal management method for cylindrical lithium-ion batteries based on flow boiling heat transfer in flexible tubes was introduced in this study. The effects of several important operating parameters, such as mass flow rate, contact area and discharge rate on the

temperature distribution and voltage distribution were discussed in detail. The purpose of this study was to reveal the thermal management performance of the proposed cooling method for a cylindrical battery pack.

2. Experimental System

2.1 System description

Fig. 1 showed the schematic diagram of experimental system in this study. The experimental system consisted of four units: a battery pack, a water-cooling cycle system, a preheating system and a data acquisition system. Driven by a peristaltic pump, the refrigerant R141b was extracted from a sealed liquid storage tank, and then it entered the flexible aluminum microchannels wound on a battery pack from the preheating section, and exchanged heat with the battery pack. Then, the refrigerant R141b was cooled in a water-cooled device and flowed back to a liquid storage tank. Six K-type thermocouples (TT-K-30-SLE, Omega, USA) were placed on the surface of each cell to measure its temperature. Two pressure sensors were used to measure the pressures of inlet and outlet of the cooling system. The mass flux of the working fluid was measured by a mass flowmeter (SITRANS F C MASS 6000). Agilent data acquisition device (Agilent 34970A) was used to collect measured data. The loads of the battery module were controlled by a charge-discharge apparatus (CT-4001-60V100A, NEWARE).

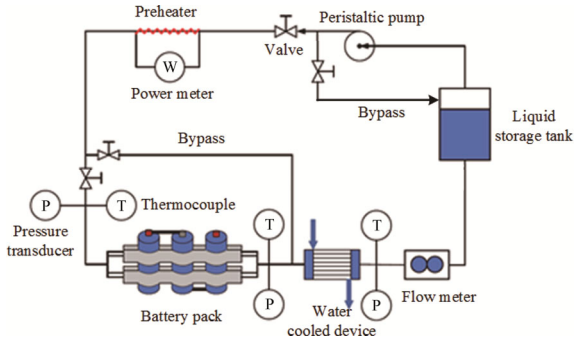

Fig. 1 Schematic diagram of the experimental apparatus

The battery used in this research was $LiFePO_4$ with a capacity of 15 Ah, a nominal voltage of 3.65 V, a diameter of 40 mm and a height of 152 mm. The refrigerant used in the experiment was R141b, and the detailed parameters of the refrigerant were shown in Table 1. In this study, the experimental uncertainties were only related to the accuracy of the single measuring devices. Table 2 summarized the accuracy of the main equipment, which provided a certain degree of reference for the reliability of the experimental results and related conclusions.

2.2 Battery pack

The batteries used in the experiment were composed of five 40152 $LiFePO_4$ batteries in series, as shown in Fig. 2(a). Two thermocouples were arranged on the surface of each battery, and the average temperature was recorded. In addition, two thermocouples were installed at the inlet and outlet of cooling microchannel plate of the battery pack to measure the temperatures of refrigerant. Aluminum microchannel plates were arranged on the side of batteries. The cross section of aluminum microchannel plate was 25.8 mm×1.0 mm, as shown in Fig. 2(b). Each microchannel plate contained 18 channels. The cross section of single channel was 0.8 mm×0.4 mm

Table 1 The physical properties of R141b

Physical property	values	Physical property	values
Molecular formula	CH_3CCl_2F	Latent heat (boiling point at 101.3 kPa)/kJ·kg^{-1}	223.0
Boiling point at 101.3 kPa/°C	32.05	Volume evaporation rate at 20°C/%	100
Critical temperature/°C	204.15	saturated liquid density at 25°C/g·cm^{-3}	1.227
Critical pressure/MPa	4.25	liquid specific heat at 25°C/kJ·kg^{-1}·°C^{-1}	1.16
Saturated vapor pressure at 25°C/MPa	0.079	critical density/g·cm^{-3}	0.43

Table 2 The accuracies of main devices in this experimental work

Device	Uncertainty
Mass flowmeter	±2%
K-type thermocouple	±0.5°C
Charge-discharge apparatus	±0.1%

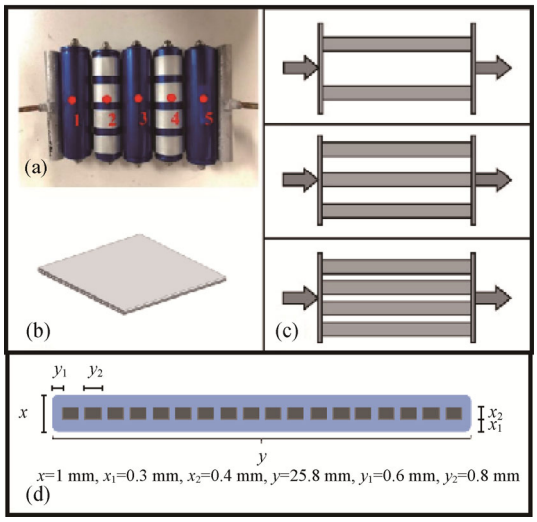

Fig. 2 Schematic diagram: (a) The battery pack system, (b) the microchannel structure, (c) cold plate structure, and (d) microchannel size data.

and the wall thickness between channel and channel was 0.6 mm. The channels longitudinal wall thickness was 0.3 mm, as shown in Fig. 2(d). Silver thermal conductivity silicone grease with a thermal conductivity of 2 W/(m·K) was coated between the battery surface and microchannel plate, and the thickness was 0.5 mm. The flexible microchannel structure could contact the cylindrical battery well. The contact area between microchannel cold plate and battery could be adjusted by changing the number of cold plates and the bending angle of cold plate. The contact center angle was 150 degrees in this paper. The structure of aluminum microchannel cold plate consisted of three parallel modes, two rows, three rows and four rows, as shown in Fig. 2(c). Different modes had different contact surface area with battery. Obviously, the contact surface area increased with the increase of row numbers.

2.3 Data reduction

Thermodynamic vapor quality was used to describe the vapor state along the flowing direction in channels and at the outlet. The heat transfer capacity of condenser was approximately equal to the sum of the latent heat of refrigerant phase change through the condenser and the sensible heat change of cooling fluid. The heat transfer capacity of condenser was calculated by

$$Q_c = C_w \cdot m_w \cdot (T_2 - T_1) = \dot{m} \cdot r + C \cdot (m - \dot{m}) \cdot (T_{out} - T_3) \quad (1)$$

where, Q_c is the heat transfer capacity of the condenser; c_w and c are the specific heat capacity of water and R141b, respectively. m_w, $\dot{m}$ and m are the mass flow rate of water, vapor mass flow of R141b and total mass flow of R141b, kg/m^3; T_1, T_2, T_{out} and T_3 are the inlet water temperature of condenser, outlet water temperature of condenser, inlet temperature of condenser refrigerant and outlet temperature of condenser refrigerant respectively, K. r is the latent heat of vaporization of R134a, kJ/kg.

The vapor quality at the outlet in channel was calculated by

$$x = \frac{\dot{m}}{m} \quad (2)$$

To simplify the heat transfer process, the heat transfer process between batteries and working fluid in the microchannels can be analogized to the heat transfer process through a fin. A lot of studies have been reported about the convective heat transfer coefficient in rectangular mini-channel with constant wall temperature [19]. The effective convective heat transfer to the cold plate was calculated considering the fin efficiency, and the heat conduction of aluminum plate and the thermal resistance of thermal grease was as given below,

$$h_{con} = \frac{1}{\frac{1}{h'} + \frac{\delta_w}{\lambda_w} + \frac{\delta_{TG}}{\lambda_{TG}}} \quad (3)$$

where, h_{con} is the heat transfer coefficient on the contact surface; h' is fin heat transfer coefficient; δ_w is wall thickness of cold plate channel; λ_w is thermal conductivity of cold plate channel; δ_{TG} is the thickness of thermal grease; λ_{TG} is thermal conductivity of thermal grease. For the microchannel structure in this paper, the effective convective heat transfer h_{con} was about 500 W/(m^2·K).

It is considered that the surface of battery without cold plate is natural convection heat transfer, so the convective heat transfer without cold plate is given below,

$$h \in [2,5] \quad \text{W/(m}^2\text{·K)} \quad (4)$$

The composite heat transfer coefficient for total battery is given below,

$$h = \frac{A_{con}}{A} h_{con} + \frac{A_n}{A} h_n \quad (5)$$

where, h is the composite heat transfer coefficient; h_{con} is the heat transfer coefficient between microchannel plate and battery surface; A_{con} is the contact area between microchannel plate and battery surface; A is the total surface area; A_n is the surface area without cold plate.

Ignore the thermal resistance of battery, the heat transfer from inside to the surface of battery can be approximated by using lumped system analysis.

$$Q_1 = \dot{\Phi}_{Li-ion} V - V \rho C_p \Delta T \quad (6)$$

where, Q_1 is the heat transferred from battery to surface to the cold plate; $\dot{\Phi}_{Li-ion}$ is the heat creation rate; V is the total volume of the battery; ρ is the battery density; C_p is specific heat capacity of the battery; ΔT is the temperature rise of the battery per unit time.

In this research, the subcooled temperature of refrigerant R141b was less than 5°C. The boiling point of refrigerant R141b at standard atmospheric pressure is 32.05°C and the temperature of refrigerant flowing into the inlet of the channel could not be lower than 27.05°C in the experiment. The convective heat transfer to the cold plate was calculated as,

$$Q_2 = h A_{con} \Delta T' \quad (7)$$

where, Q_2 is the convective heat transfer to the cold plate; A_{con} is the contact area between the microchannel plate and the battery surface; $\Delta T'$ is the difference between the cold plate wall temperature and the fluid temperature of refrigerant R141b.

The ratio of the contact area between microchannel plate and battery surface to the total side surface of battery was calculated as follows,

$$a = \frac{A_{con}}{A_s} \quad (8)$$

where, a is the ratio of the cooling area of battery by the microchannel plate (A_{con}) and the total side surface of battery (A_s). When row number was 2 (n=2), the ratio

was 14%. For row number being 3 (n=3), the ratio was 21%, and the ratio was 30% for row number being 4 (n=4).

3. Results and Discussions

The thermal behavior and electrochemical behavior of the battery pack under this thermal management mode were compared with that under non-cooling mode. During the experiments, the ambient temperature was 25°C. The battery module consisted of five batteries connected in series. The cut-off condition of constant current discharge was the voltage of battery module reached 12.5 V or the voltage of one battery reached 2.5 V first.

In particular, the maximum temperature and the temperature uniformity were discussed at different discharge rates. The thermal behavior of battery pack with different cooling areas was analyzed. The effects of cooling areas on the temperature performance of battery module were discussed in detail. The temperature performance was presented with the maximum temperature and temperature difference on the battery pack.

3.1 Thermal and electrochemical properties without cooling system

3.1.1 Thermal behavior

The battery module was discharged at 3C and 5C without cooling system. Fig. 3 shows the average temperature and temperature difference of battery surface without cooling system. The temperature difference referred to the temperature difference on the surface of a single battery. The maximum temperature difference was the selected largest value from the tested five batteries. The average temperature increased from 25.6°C to 51.1°C and the highest temperature difference was 10.2°C at 3C discharge rate. The average temperature increased from 24.8°C to 59.7°C and the highest temperature difference was 13.2°C at 5C discharge rate. The results showed that the temperature of battery surface increased with the increase of discharge rate, in other words, the larger the discharge current was, the faster the temperature rose. The temperature rising rate was about 0.05 K/s in the first 400 seconds. However, the operating temperature and temperature difference for a single battery or a battery module should be in the range of 20°C to 40°C and 5°C, respectively. So, it is necessary to design an appropriable battery thermal management system.

3.1.2 Discharge curves

The output voltage and discharge capacity distribution of the battery module were shown in Fig. 4. At the same ambient temperature, the output voltage at 3C was much higher than that at 5C. The discharges ended early because the voltage of one battery reached 2.5 V first.

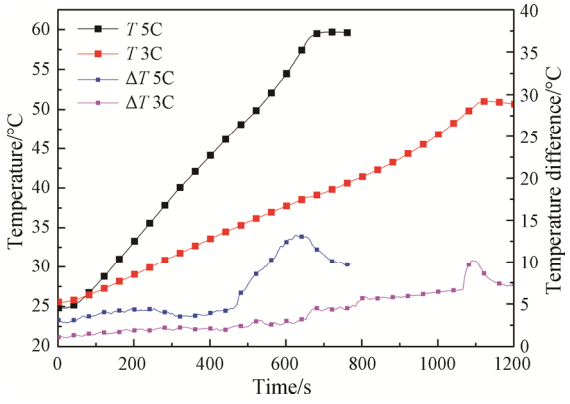

Fig. 3 Temperature distribution of the battery surface at 3C and 5C without cooling system

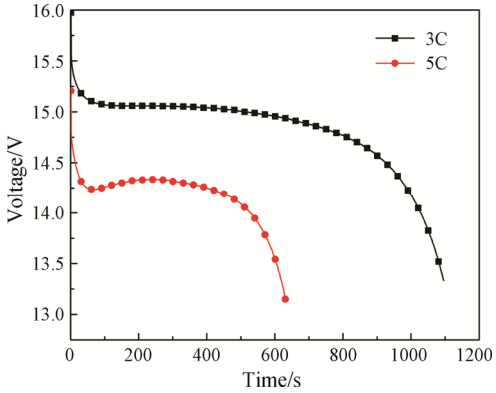

Fig. 4 The output voltage and discharge capacity distribution of battery module at 3C and 5C

3.2 Effects of mass flow rate

3.2.1 Thermal behavior

Inlet mass flow rate played an essential role in cooling battery module. In this study, the inlet mass flow rate increased from 0 kg/h to 10 kg/h. In order to more comprehensively cover the range of operating conditions and reflect the differences in the characteristics of phase change effect, at the largest selected mass flow value, the refrigerant in the microtubes would maintain the single-phase heat transfer state. At other three mass flow values, the flow boiling heat transfer would occur in microtubes corresponding to different outlet vapor quality. Thus, the relevant optimal heat transfer state might be determined. The battery was discharged at 5C rate and the row number of aluminum block was 4. The surface heat transfer coefficient under this structure was 137 W/(m^2·K).

Fig. 5 demonstrated the temperature distribution of cold plates and the vapor qualities at the outlet. The temperature variation on cold plate depended on the temperature and flow pattern of the refrigerant in cold plate. When the refrigerant in cold plate was in single-

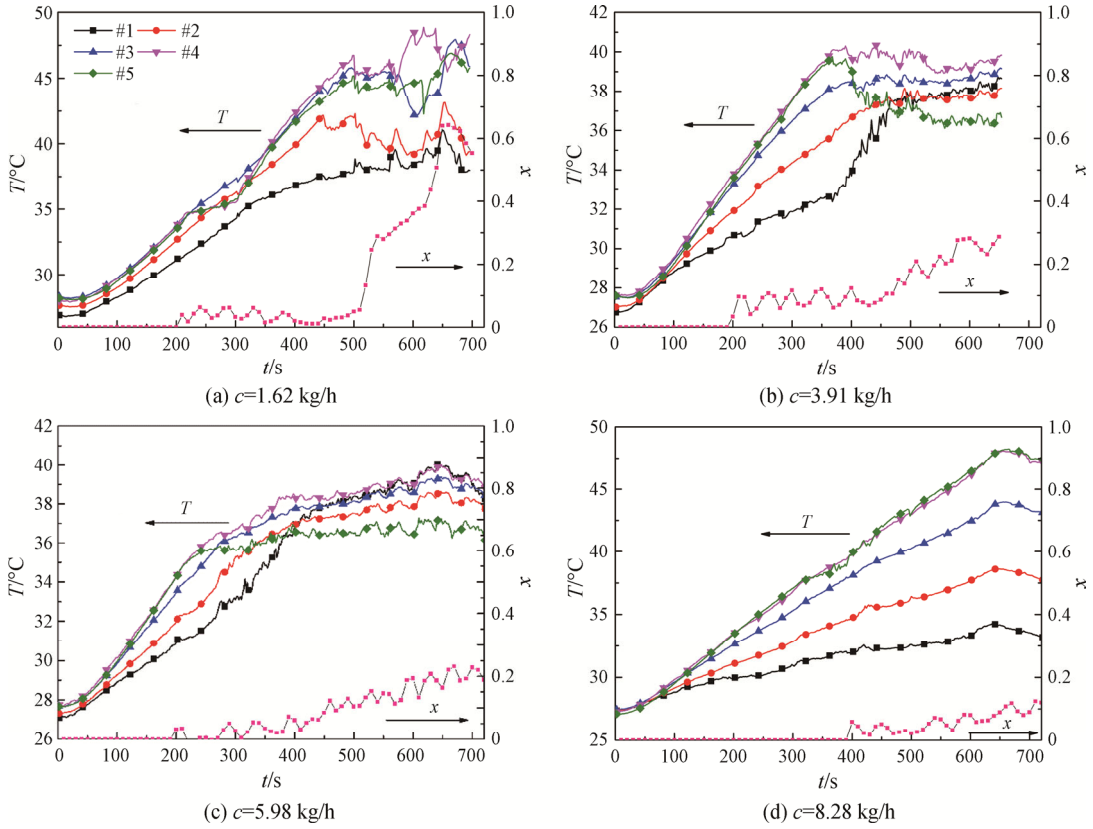

Fig. 5 Temperature distribution of the battery module and the qualities change of outlet (n=4)

phase flow, the surface temperature of cold plate increased with the increase of the refrigerant temperature, and the temperature gradient was basically unchanged. When the fluid in the microchannels became two-phase flow, the surface temperature gradient of cold plate also changed significantly. And the wall temperature of cold plate rose slowly and tended to balance, and no longer rose or even dropped at low flow rates.

In Fig. 5, with the depth of discharge of battery, the temperature gradient on cold plate changed significantly, meaning that the refrigerant in channels changed from a single-phase flow to a two-phase flow. At different inlet mass flow rate, the change of temperature gradient on cold plate depended on location. When the inlet mass flow rate was 1.62 kg/h, 3.91 kg/h and 5.98 kg/h, the refrigerant in microchannel basically entered the flow boiling at the first 500 seconds. Since the heat generation rate increased during the discharge process, it means that the heat generation in battery increased, and the heat absorbed by the refrigerant also increased, so the vapor quality of outlet also increased. When the inlet mass flow rate was 8.28 kg/h, the refrigerant in channel kept in single-phase flow all the time.

Table 3 illustrated the relevant data at different flow rates, including c=0, 1.62, 3.91, 5.98, 8.28, 10.00 kg/h. The batteries were discharged at 5C rate. When the mass flow rate was 5.98 kg/h, the highest temperature and the lowest temperature of battery surface were 47.91°C and 43.3°C, respectively. The temperature and the temperature difference in this situation were the lowest. It was because that the main flow pattern of refrigerant in channels was in a single-phase flow at high mass flow rates, and the heat taken away was less. The maximum temperature and the minimum temperature were relatively higher, but the temperature difference was reduced. When the flow rates were between 1.62 and 8.28 kg/h, the vapor qualities of refrigerant were 0.63, 0.29, 0.23, 0.08, and the refrigerant changed from single-phase flow to flow boiling, so more heat was taken away. However, it can also be seen that the surface temperature of battery could not fulfil the safe operation conditions of battery at 5C discharge rate. According to the previous calculation, it is found that the heat quantity Q_c was less than that released by battery Q_1. To control the temperature within the appropriate operating range, it was necessary to increase the number of cold plates.

With high discharge rate, the uniformity of the surface temperature of battery will be improved due to the existence of thermal management. The difference in surface temperature of the battery decreased first as the mass flow rate of refrigerant increased. When the mass flow rate was greater than 8.28 kg/h, the temperature

difference slightly increased. This was because the refrigerant in channels was single-flow, and its cooling effect deteriorated.

3.2.2 Discharge curves

Fig. 6 demonstrated the output voltage and discharge capacity distribution of battery module at 3C and 5C discharge rates. Because of the electrochemical reaction and the Ohmic effect of battery, the temperature of battery rose during the charging and discharging process. Conversely, in a single charge and discharge process, the battery operating temperature directly affected the macroscopic electrochemical characteristics of battery, including the output voltage and capacity, so the temperature was an important factor in determining the rate of battery capacity decay and safety. Comparing the output voltage and discharge capacity of battery under different mass flow rates, it was indicated that the output voltage and discharge capacity of battery increased first and then decreased with the increase of mass flow rates, and both of them exhibited the best characteristics when the mass flow rate was 6 kg/h. It could be concluded that the electrochemical characteristics of battery at the mass flow rate of 6 kg/h was optimal.

Table 3 The Parameters at different flow rates (n=4)

c/kg·h^{-1}	Re	x	T_{max}/°C	T_{min}/°C	ΔT/°C
0			62.47	51.865	10.605
1.62	50.54	0.63	52.62	47.17	5.45
3.91	101.08	0.29	49.64	44.079	5.561
5.98	151.62	0.23	47.91	43.294	4.616
8.28	202.16	0.08	49.29	44.647	4.643
10.00	252.70	0	52.87	47.208	5.662

3.3 Effects of the cooling area

Since the cooling area played an important role in the battery thermal management, the effects of the inlet mass flow rate and cooling area on the average temperature and temperature difference were studied on the cooling performance, as shown in Fig. 7. The battery was discharged with 3C rate.

The aluminum channel plate cooling area for each cell was consistent. As shown in Fig. 7(a), the row number of aluminum channel plate was changed from 2 to 4, and the inlet mass flow rate was increased from 0 kg/h to 10 kg/h. For the row number of aluminum block being 2, the maximum temperature of battery module was dropped from the highest 49.3°C to the lowest 45.5°C at 6 kg/h. The maximum temperature of battery module was

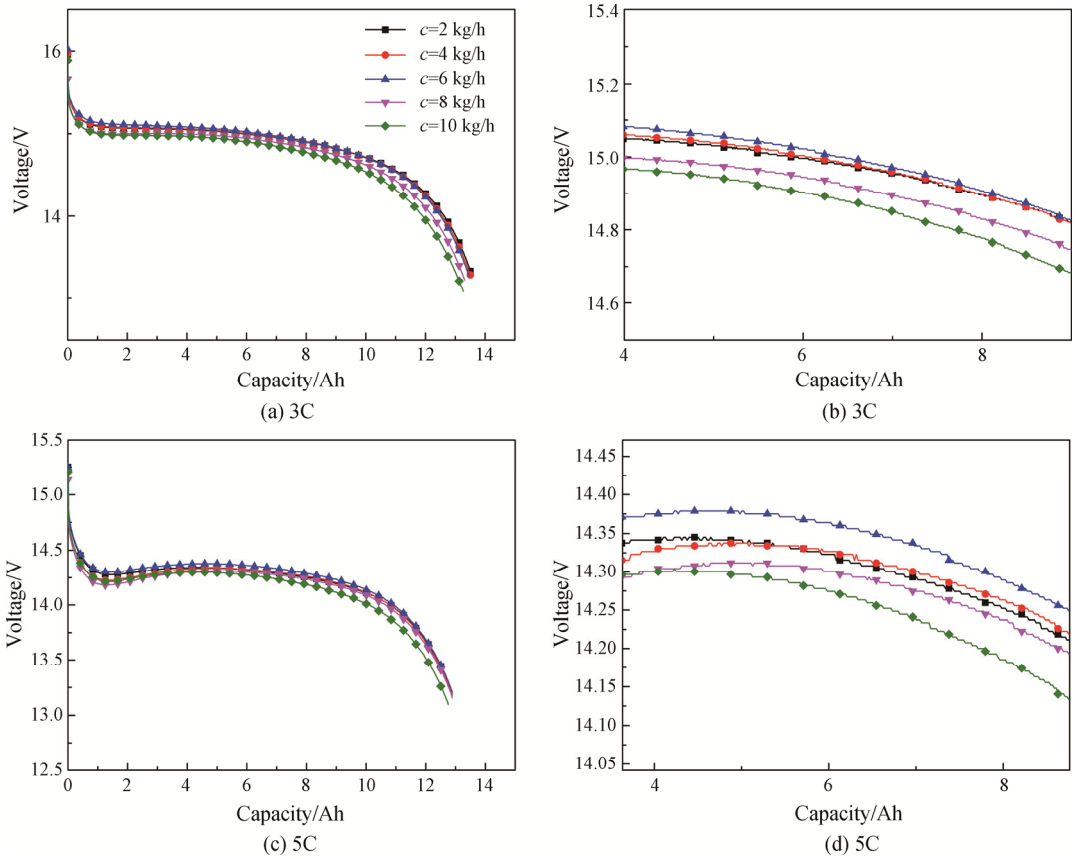

Fig. 6 The output voltage and discharge capacity distribution of battery module

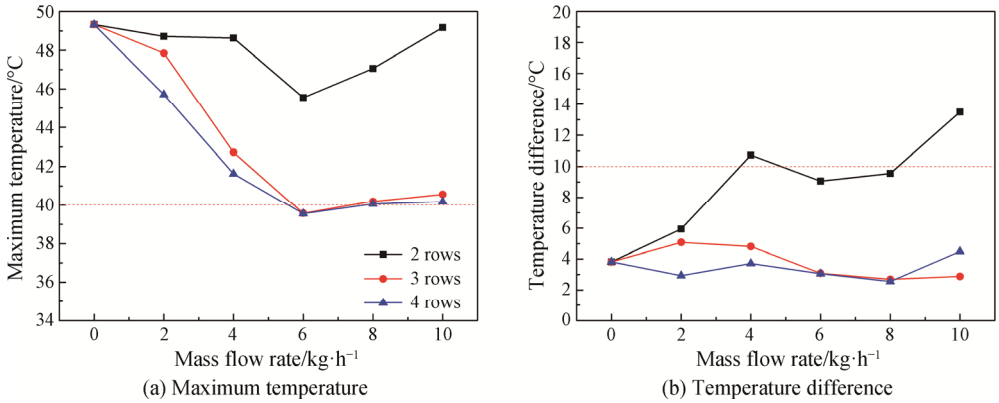

Fig. 7 The maximum temperature and temperature difference of the battery module at different inlet mass flow rate

dropped from the highest 49.3°C all the time, and the minimal value 39.5°C of average temperature of the battery module was reached when the row number was 4, and the cooling performance was the best.

It was known that the maximum temperature difference should be no more than 5°C in a single battery or a battery module. Under low discharge rate such as 3C, the battery surface temperature difference itself was not high. It could be concluded that the inlet mass flow rate must be controlled within a reasonable range. The best cooling performance was performed when the inlet mass flow rate was 6 kg/h to 8 kg/h, whatever the row number was 3 and 4. At these conditions, the outlet vapor quality of microtubes maintained the optimal value range, where the flow boiling state was sufficient and can be guaranteed to be far below the dry out state. Therefore, both the temperature uniformity and the heat dissipation effect of the batteries were in good condition. While the row number was 4, the temperature difference was kept under 5°C expect the inlet velocity of 10 kg/h. It meant that the temperature difference increased when the inlet mass flow rate was more than or equal 10 kg/h. The results also proved that higher mass flow rate had a negative effect on cooling performance with constant cooling area. At higher mass flow rate, the single-phase heat transfer was the dominating mechanism for the thermal management of batteries, thus, the good temperature uniformity and efficient heat dissipation brought by the flow boiling heat transfer technology cannot be reflected since the extremely lower outlet vapor quality. The temperature would increase along the flow direction of microtubes. At all flow rates, the temperature uniformity of battery increased with the increase of the number of cold plates. This was because the effective heat transfer area on the surface increased with the increase of the number of cold plates, so the battery temperature difference decreased.

4. Conclusions

In this paper, a novel liquid cooling based thermal management system for flexible cylindrical lithium-ion battery module was proposed. The flexible microchannel structure could make the contact area with cylindrical battery increase. The contact area between the micro-channel cold plate and the battery could be adjusted by changing the number of cold plates and the bending angle of the cold plate. Main conclusions were follow:

(1) With the high discharge rate, the maximum surface temperature and uniformity of cell surface temperature would be advanced under the condition of phase change heat transfer. When the outlet dryness was between 0.2–0.3, the flow boiling heat transfer in microchannels gave a good contribution for thermal management, and the maximum surface temperature and surface temperature difference were the lowest.

(2) With discharge rates of 3C and 5C, the macro-electrochemical characteristics of batteries were affected by the mass flow rate in microchannels. With the increase of mass flow rate, the output voltage of the battery increased first and then decreased, but the discharge capacity of battery decreased with the increase of flow rate.

(3) For low discharge rate, with the increase of contact area between battery and cold plate, the difference between surface temperature and surface temperature decreased. At 3C discharge rate, the cooling area ratio of 21% could meet the stable and safe operation temperature range of battery. However, when the cooling area ratio was 30% at 5C discharge rate, it could not meet the requirements of batteries. It was necessary to increase the contact area to achieve better cooling effect.

Acknowledgments

This research was supported by National Natural Science Foundation of China (No. 51776015).

References

[1] Pesaran A.A., Battery thermal management in EV and

HEVs: issues and solutions. Battery Man, 2001, 43: 34–49.

[2] Scrosati B., Garche J., Lithium batteries: Status, prospects and future. Journal of Power Sources, 2010, 195: 2419–2430.

[3] Goodenough J.B., Park K.S., The Li-ion rechargeable battery: a perspective. Journal of the American Chemical Society, 2013, 135: 1167–1176.

[4] Wang Q., Ping P., Zhao X., Chu G., Sun J., Chen C., Thermal runaway caused fire and explosion of lithium ion battery. Journal of Power Sources, 2012, 208: 210–224.

[5] Drake S.J., Martin M., Wetz D.A., Ostanek J.K., Miller S.P., Heinzel J.M., Jain A., Heat generation rate measurement in a Li-ion cell at large C-rates through temperature and heat flux measurements. Journal of Power Sources, 2015, 285: 266–273.

[6] Li X., He F., Ma L., Thermal management of cylindrical batteries investigated using wind tunnel testing and computational fluid dynamics simulation. Journal of Power Sources, 2013, 238: 395–402.

[7] Zhang Z., Jia L., Zhao N., Yang L., Thermal modeling and cooling analysis of high-power lithium ion cells. Journal of Thermal Science, 2011, 20: 570–575.

[8] Mohammadian S.K., Zhang Y., Thermal management optimization of an air-cooled Li-ion battery module using pin-fin heat sinks for hybrid electric vehicles. Journal of Power Sources, 2015, 273: 431–439.

[9] Sun H., Dixon R., Development of cooling strategy for an air cooled lithium-ion battery pack. Journal of Power Sources, 2014, 272: 404–414.

[10] Zhao R., Gu J., Liu J., An experimental study of heat pipe thermal management system with wet cooling method for lithium ion batteries. Journal of Power Sources, 2015, 273: 1089–1097.

[11] Rao Z., Huo Y., Liu X., Experimental study of an OHP-cooled thermal management system for electric vehicle power battery. Experimental Thermal and Fluid Science, 2014, 57: 20–26.

[12] Rao Z., Wang S., Wu M., Lin Z., Li F., Experimental investigation on thermal management of electric vehicle battery with heat pipe. Energy Conversion and Management, 2013, 65: 92–97.

[13] Park Y., Jun S., Kim S., Lee D.H., Design optimization of a loop heat pipe to cool a lithium ion battery onboard a military aircraft. Journal of Mechanical Science and Technology, 2010, 24: 609–618.

[14] Khateeb S.A., Amiruddin S., Farid M., Selman J.R., Al-Hallaj S., Thermal management of Li-ion battery with phase change material for electric scooters: experimental validation. Journal of Power Sources, 2005, 142: 345–353.

[15] Rao Z., Huo Y., Liu X., Zhang G., Experimental investigation of battery thermal management system for electric vehicle based on paraffin/copper foam. Journal of the Energy Institute, 2015, 88: 241–246.

[16] An Z., Jia L., Li X., Ding Y., Experimental investigation on lithium-ion battery thermal management based on flow boiling in mini-channel. Applied Thermal Engineering, 2017, 117: 534–543.

[17] Qian Z., Li Y., Rao Z., Thermal performance of lithium-ion battery thermal management system by using mini-channel cooling. Energy Conversion and Management, 2016, 126: 622–631.

[18] An Z., Jia L., Ding Y., Dang C., Li X., A review on lithium-ion power battery thermal management technologies and thermal safety. Journal of Thermal Science, 2017, 26: 391–412.

[19] An Z., Shahb K., Jia L., Ma Y., A parametric study for optimization of minichannel based battery thermal management system. Applied Thermal Engineering, 2019, 154: 593–601.